Analysis of the Pyramidalization of the Peptide Group Nitrogen: Implications for Molecular Mechanics Energy Functions

Berit E. Mannfors, Noemi G. Mirkin, Kim Palmo, and Samuel Krimm*

Biophysics Research Division and Department of Physics, University of Michigan, Ann Arbor, Michigan 48109

Received: August 27, 2002; In Final Form: October 31, 2002

Pyramidalization at the peptide group nitrogen atom is analyzed using *N*-methylacetamide (NMA) as a model molecule. Mutually orthogonal peptide CN torsion and NH out-of-plane bend coordinates are necessary for a correct description of the energetics of nonplanar deformations of the peptide group. Using such coordinates, ab initio calculations at the MP2/6-31++G(d,p) level of theory show that the energy minimum of the NH out-of-plane bend angle shifts significantly away from zero for nonzero CN torsion angles. Not being due to nonbonded interactions alone, this energy behavior needs to be taken explicitly into account in molecular mechanics force fields. By use of different schemes for calculating potential-derived atomic charges, the charge distribution of NMA was also investigated in connection with the pyramidalization. Large variations in the charges were found as a function of the NH out-of-plane angle. These could not be reproduced only by polarization through the (molecular mechanics) electric field. An enhanced electrostatic model, using geometry-dependent charges (charge fluxes) is shown to provide a satisfactory physical description of this effect.

1. Introduction

For realistic molecular modeling of proteins, such as molecular mechanics (MM) and molecular dynamics (MD) simulations, a good physical description of the properties of the peptide group is of crucial importance. Due to the fact that this group is polar, its electrostatic properties play a dominant role in all inter- and intrachain interactions. In addition, the dynamic properties of the peptide group itself are important, these being largely determined by valence interactions. An accurate MM valence model is thus needed, for example to describe the motion of the amide hydrogen in terms of the NH bond vector in MD simulations, which is central to NMR investigations of protein dynamics.[1] Modeling to aid Raman-[2] and IR-based[3] vibrational spectroscopic studies also requires a very realistic representation of the valence properties. The MM spectroscopically determined force fields (SDFFs) that we are developing are specifically designed to fulfill such strict demands on accuracy needed in these types of applications.

Among important valence terms in the peptide group are the out-of-plane deformations, which cannot be described properly with the standard redundant set of torsion and out-of-plane bend (ob) coordinates used in all conventional MM force fields. The standard set includes all dihedral angles as separate coordinates, which each carry potential energy. In combination with the two ob coordinates, this means that six coordinates are used to describe a three-dimensional space. It has, in fact, been pointed out that the redundant representation is inappropriate and that the torsion coordinate of any sp^2-sp^2 bond should be orthogonal to the associated ob coordinates.[4−10] Otherwise, deformation of an ob coordinate will also register as a torsion deformation. Nevertheless, with the exceptions of our alkene SDFF[6] and some earlier force fields,[5,7,8] such appropriate coordinates have not been implemented in current force fields. A suitable nonredundant sp^2-sp^2 torsion coordinate measures the angle between the π orbitals rather than any (or all) of the dihedral angles involved. This issue is of direct significance for describing peptide energetics and dynamics, since, for example, out-of-plane motion of the NH bond vector is governed by a much smaller force constant than is CN torsion (when using nonredundant coordinates). Inappropriate mixing of these particular coordinates inevitably causes incorrect energetics descriptions of them. It also leads to incorrect dynamics, as evidenced by large errors in the calculated NH ob vibrational frequencies (ref 10, supplementary material).

As part of our efforts to develop a peptide SDFF, we encountered additional complications. For example, even with attention to this coordinate orthogonality, we could not obtain consistent SDFF-transformed[11] NH ob intrinsic geometry parameters from different conformations of glycine and alanine dipeptides (i.e., the intrinsic parameter was not transferable), and then, of course, we were unable to properly reproduce the ab initio dipeptide geometries with such a force field. This led us to study more thoroughly the properties of the peptide group, with the goal of improving the SDFF by incorporating important new physically significant features that have been neglected, especially with regard to pyramidalization at the nitrogen atom.

Using *N*-methylacetamide (NMA) as a model molecule, we present here the results of an ab initio investigation of the potential energy associated with peptide NH ob deformation as a function of the peptide CN torsion angle, using mutually orthogonal torsion and ob coordinates. From these results we show that a modified description of the SDFF NH ob potential energy is indeed required (beyond the use of orthogonal internal coordinates). In addition, most MM force fields use a Coulomb potential with fixed atomic point charges to describe electrostatic interactions. However, it is important not to neglect the possibility that the charges may depend on conformation, and in this work we show that NH ob deformation causes significant changes in the atomic charges, these being determined from the electric potential around the NMA molecule (i.e., potential-derived (PD) charges[12]). In this paper we have applied two

* To whom correspondence should be addressed. Telephone: (734) 763-8081. Fax: (734) 764-3323. E-mail: skrimm@umich.edu.

10.1021/jp0219606 CCC: $25.00
Published on Web 02/21/2003

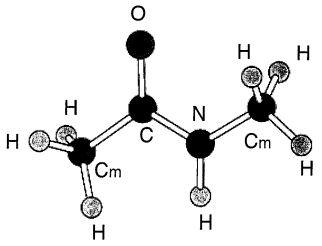

Figure 1. Notation of the atoms in NMA.

TABLE 1: NH Out-of-Plane Bend Angle γ (in deg) as a Function of CN Dihedral Angles, ω_1 and ω_2, at a Fixed Peptide CN (Bell) Torsion Angle ω^a of 15°

$\omega_1{}^b$	$\omega_2{}^b$	γ
35	−5	−35.6
30	0	−26.4
25	5	−17.5
20	10	−8.7
15	15	0.0
10	20	8.7
5	25	17.5
0	30	26.4
−5	35	35.6

[a] $\omega = (\omega_1 + \omega_2)/2$. [b] ω_1 and ω_2 correspond to the $OCNC_m$ and C_mCNH dihedral angles, respectively.

different MM electrostatic models, a nonpolarizable and a polarizable one, to account for the charge variations. Using the nonpolarizable model, which implicitly includes polarization effects, we have tried to reproduce these changes by charge fluxes (i.e., including structure dependence in the charges). In the context of our polarization model,[13,14] we have investigated whether polarization alone can explain the charge variations. In the most complete MM model used here, we apply both polarizability and charge fluxes to explain the structure dependence of the charges.

2. Methods

The quantum mechanical (QM) calculations in this work were done at the MP2/6-31++ G(d,p) level of theory using the GAUSSIAN 98[15] and GAMESS[16] software packages. The QM level is the same as the one used in our previous study of NMA electrostatics,[14] higher levels, in the development of MM energy functions, being restricted by the need to treat, in a consistent way, both small and large model systems with the same QM method and basis set. GAUSSIAN 98 was used for potential energy calculations and for computation of the CHELPG[17] PD atomic charges. GAMESS was used to compute the electric potential on various planes through the NMA molecule, as needed in our own procedure for optimizing PD charges,[13] and for calculating the PD charges according to the geodesic point selection scheme by Spackman.[18] All MM parameter optimizations were done with the SPEAR program.[19]

The QM potential energy and the PD atomic charges were calculated for NMA as a function of the Wilson[20] NH ob angle for various deformations of the peptide CN torsion angle. As nonredundant CN torsion coordinate we use Bell's torsion angle,[21] in this case defined as the average of the $OCNC_m$ and C_mCNH dihedral angles (Figure 1). These angles were set to values that yielded the desired range of NH ob (from −45° to 45°) and CN torsion (from −90° to 90°) deformations. As an example, Table 1 illustrates how the components of the peptide CN Bell torsion coordinate, ω, determine the NH ob angle, γ, for a 15° CN torsion angle. To avoid interference from other deformations, three additional constraints were applied: for the *N*-methyl group one CNC_mH dihedral angle was held at 180°, and for the *C*-methyl group one NCC_mH dihedral angle was held at 0°. The CO ob angle was also constrained to be 0°.

Our MM electrostatic model basically consists of atomic charges and dipoles.[13] Polarization is taken into account using induced charges and dipoles.[13,14] In addition, geometry dependence can be accounted for by charge and dipole fluxes.[22,23] In this work we use charge fluxes to describe changes in the charge distribution due to NH ob deformation. The charge fluxes are based on a linear model;[22] i.e., the atomic charges are allowed to vary linearly with deformations of internal coordinates. To keep the molecule neutral, the charge fluxes always pertain to bonds, so that if one atom of a bond gains positive charge, the other atom of the bond simultaneously gains the same amount of negative charge. This is implemented in SPEAR by using bond increments both for fixed charges and for charge fluxes.[22] Thus, the fixed charge on atom i is given by

$$q_i = \sum_b q_{ib} \tag{1}$$

where q_{ib} is the bond charge increment (BCI) of bond b, and the summation runs over all bonds that contain atom i. Similarly, the charge flux in bond b is given by

$$\Delta q_b = \sum_j a_{bj}(r_j - r_{j0}) \tag{2}$$

where r_{j0} is the reference value of the internal coordinate j and the a_{bj}'s are the charge flux parameters. For a torsion coordinate χ_j, $(r_j - r_{j0})$ is replaced by $\cos \chi_j$. The total charge on atom i is obtained by adding Δq_b to q_i for all bonds that contain atom i.

The electrostatic parameters are optimized to the electric potential rather than to other QM observables, such as the electron density or the electric field, because the electric potential is more closely related to the electrostatic potential energy.[13] For the purpose of applying various electrostatic models[14] in NMA, we calculated the electric potential on seven different planes through the molecule for each ob configuration. Each plane contained about 6000 points. In addition, we used 45 geodesic layers around the NMA molecule. The layers also contained about 6000 points altogether. The number of layers was chosen higher than the default value (4) suggested by Spackman[18] because we wanted to include more points farther from the molecule to better probe the long-range electrostatic properties. However, because the number of points per layer is constant, the Spackman scheme yields a higher density of points closer to the molecule than farther away. On the other hand, the planes through the molecule, which we primarily utilize for parameter optimization, contain equally spaced points, so the combination of planes and layers covers the space around the molecule in a reasonable fashion, and with very little inherent dependence on external rotation and translation of the molecule (or the coordinate axes). Such dependence has been shown to be significant in schemes relying on Cartesian grids,[18,24] including CHELPG.

3. Results and Discussion

In the following, the results concerning the valence potential energy and the variations in the electric potential as a function of pyramidalization of the structure around the peptide nitrogen atom are discussed separately.

3.1. Valence Potential for Nitrogen Pyramidalization in the Peptide Group. The peptide group in NMA is known to be planar at the energy minimum,[25] but the geometry in peptide chains may deviate significantly from planarity even in low-

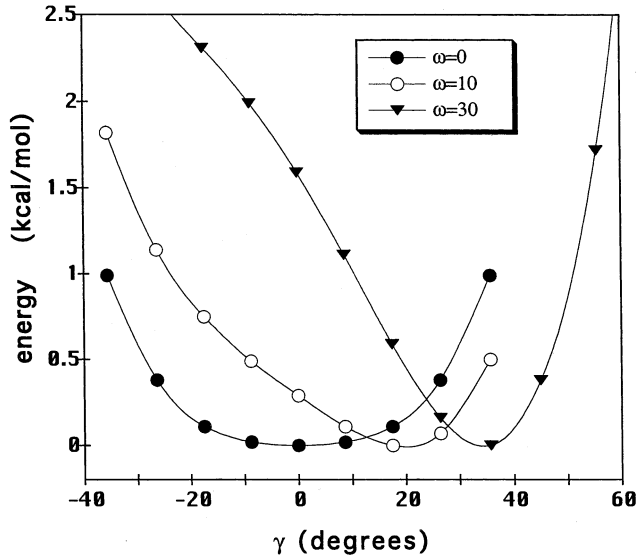

Figure 2. Energy of NMA as a function of the NH out-of-plane angle γ for three different peptide CN (Bell) torsion angles ω. The offsets in the energies with respect to $\omega = 0°$ are 0.46 kcal/mol for $\omega = 10°$ and 4.76 kcal/mol for $\omega = 30°$.

energy conformations.[26−28] As mentioned above, when using conventional force fields in which the peptide CN torsion and NH ob (and C═O ob) coordinates form a redundant set, the NH ob energetics become severely misrepresented. With nonredundant torsion and ob coordinates the energetics can be properly described, but appropriate force constants and geometry parameters are of course still needed. All current force fields contain fixed force constants and intrinsic geometry parameters for ob deformations. We now take into account the possibility that the parameters associated with NH ob may depend on conformation, i.e., on the peptide CN torsion angle.

The ab initio potential energy was computed for NH ob deformations in the range −45° to 45° as a function of the peptide CN Bell torsion angle in the range −90° to 90°. These calculations revealed asymmetry in the NH ob energy curves for nonzero values of the CN torsion angle. An example of this is shown in Figure 2 for CN torsion angles 0°, 10°, and 30°. For easier comparison, the energy curves are offset by the minimum energy relative to $\omega = 0°$. Clearly, the NH ob energy minimum occurs at larger deformations with increasing torsion angle, indicating that the planarity around the nitrogen atom is not maintained with peptide CN rotation. Additional ab initio calculations confirmed that the behavior is essentially the same when the NH group is hydrogen bonded to a water molecule. SDFF test calculations using our fixed charge model[14] indicate that the effect cannot be accounted for by the nonbonded interactions. The intrinsic geometry parameter γ_0 for NH ob in the SDFF can therefore no longer be assumed to be a constant. Instead, preliminary results[29] indicate that the behavior of γ_0 can be described by the function

$$\gamma_0 = c \sin a\,\omega \qquad (3)$$

where ω is the peptide CN Bell torsion angle and c and a are constants. This effect must be included in MM force fields if correct peptide dynamics is to be obtained.

We also did ab initio calculations to find the minimum-energy value of ω for a few different fixed deformations of γ (using the same constraints as before). The resulting deformations of ω were very small (<5°).

3.2. Electrostatic Model for Nitrogen Pyramidalization in the Peptide Group. We have recently studied MM electrostatic models extensively[13,14,30] and found that, in many cases, fixed atomic charges are insufficient to properly account for important interactions where electrostatic features dominate.[13,14] As a relatively simple extension of the point charge model, we have incorporated atomic dipoles. In some cases, including them yields much better agreement with ab initio electric potentials,[13] although this was not found to be the case for NMA.[14] In addition, we have developed polarizability models,[13,14] one of which allows intramolecular charge flow. For example, our NMA monomer-optimized polarizability models excellently reproduce, without modification, the ab initio electric potentials, dipole moments, and polarizability tensors of three different hydrogen-bonded configurations of the NMA dimer.[14] In these investigations the main emphasis was on intermolecular interactions. We now turn to intramolecular electrostatic effects.

The initial ab initio study of the valence NH ob potential showed significant changes in the CHELPG PD charges of the peptide group, indicating that they cannot be assumed to remain unchanged with pyramidalization at the nitrogen atom. We therefore decided to systematically investigate how the atomic charges vary as a function of the NH ob deformation at different moderate (from −30° to 30°) CN torsion angles. To check that the charge variations were not an artifact of the CHELPG scheme, PD charges for some cases were also calculated with the Spackman scheme. Different numbers of layers around the molecule with different numbers of points per layer were tested, but the charges were very close to each other in each case. Although the Spackman charges were somewhat different from the CHELPG ones, the variations of the charges as a function of the NH ob deformation were similar, the CHELPG variations being smaller. From this we concluded that, at least for the present study, the trends of the CHELPG charges could be used as reference data.

The calculations of the CHELPG charges as a function of the NH ob angle (Table 2) show that the charges on the *C*-methyl hydrogen and carbonyl oxygen atoms vary only slightly, at most about 0.01 e, whereas the carbonyl carbon, nitrogen, and *N*-methyl carbon atoms experience the largest changes. Also the *C*-methyl carbon and two of the *N*-methyl hydrogen atoms exhibit charge variations of about 0.05 e. The largest relative changes occur for the *N*-methyl hydrogen atoms. The charge variations are about the same for positive and negative NH ob angles, as seen from the symmetry (with respect to $\gamma = 0°$) of the data shown for the nitrogen atom in Figure 3. Further, the charges of all atoms in NMA are found to be less sensitive to the CN torsion angle (in the range of −30° to 30°) than to the NH ob angle.

In developing an MM model to reproduce these ab initio results, we first applied our previous charge model with fixed charges[14] but, as expected, the ab initio electric potentials were not well reproduced for the deformed structures (see Tables 3 and 4 and Figure 4). The weighted relative root-mean-square (wrrms) deviations strongly increase with increasing ob deformation and are, for example, 8.6% for 26.4° and 15.5% for 45° NH ob deformation, compared to 4.8% for the planar case. A set of average charges could of course be optimized, but this would not be ideal for any configuration. Neither could the changes in the charges be explained by polarization (note that our polarizability model allows charge flow in a molecule). In fact, inclusion of polarizability did not give much better results than the fixed charge model, the wrrms deviation being, for example, 14.6% for the 45° deformation. Thus, there are cases where charge fluctuations must be directly attributed to defor-

TABLE 2: MP2/6-31++G(d,p) CHELPG Charges (in electrons) of NMA at Different NH Out-of-Plane Angles γ for a 15° Peptide CN (Bell) Torsion Angle

atom[a]	$\gamma = 0°$	$\gamma = 8.7°$	$\gamma = 17.5°$	$\gamma = 26.4°$	$\gamma = 35.6°$	$\gamma = 45.0°$
C_m (*C*-methyl)	−0.512	−0.517	−0.519	−0.551	−0.536	−0.562
H	0.146	0.145	0.145	0.152	0.148	0.155
H	0.139	0.139	0.140	0.146	0.139	0.142
H_{ip}	0.111	0.110	0.109	0.118	0.115	0.123
C	0.773	0.798	0.811	0.844	0.864	0.890
O	−0.585	−0.591	−0.592	−0.594	−0.594	−0.594
N	−0.600	−0.624	−0.655	−0.697	−0.723	−0.743
H	0.326	0.334	0.343	0.352	0.354	0.353
C_m (*N*-methyl)	0.032	0.034	0.077	0.122	0.133	0.155
H_{ip}	0.057	0.057	0.044	0.032	0.030	0.024
H	0.055	0.059	0.055	0.051	0.055	0.055
H	0.060	0.057	0.043	0.026	0.016	0.002

[a] C_m denotes sp^3 carbon and H_{ip} refers to the *C*-methyl and *N*-methyl hydrogens for which the C_mH bonds were constrained to be coplanar with the CN bond.

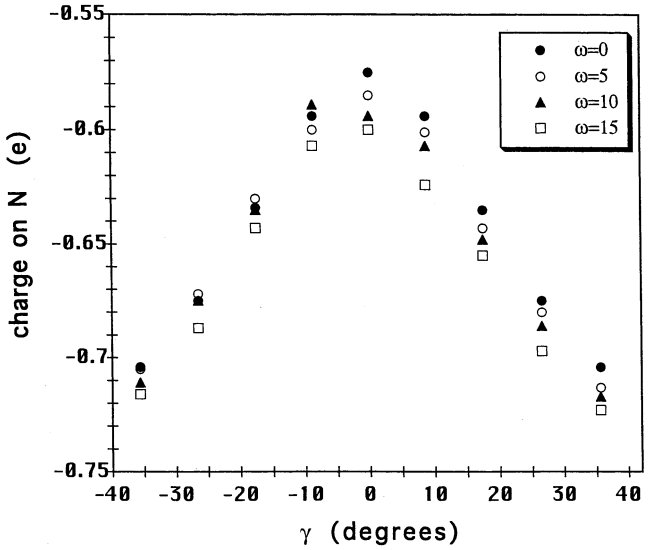

Figure 3. MP2/6-31++G(d,p) CHELPG charge on the nitrogen atom of NMA as a function of the NH out-of-plane angle γ for four different peptide CN (Bell) torsion angles ω.

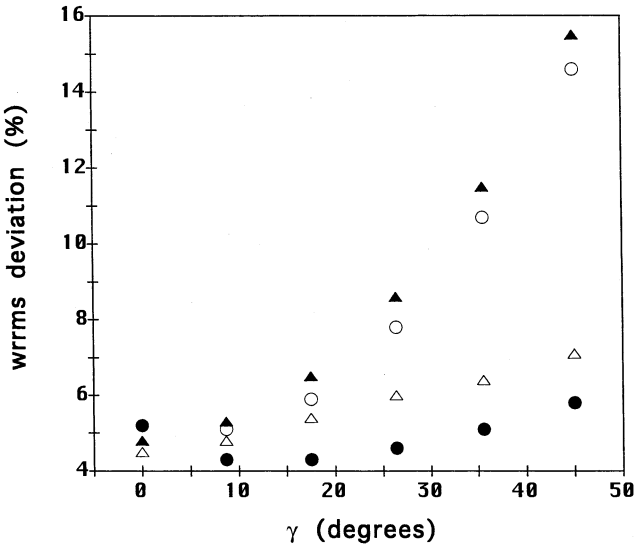

Figure 4. Weighted relative root-mean-square deviations of the MM fit to the MP2/6-31++G(d,p) electric potential of NMA as a function of the NH out-of-plane angle γ. The different electrostatic models are denoted as follows: ▲, (nonpolarizable) fixed charge model;[14] ○, polarizable model;[14] △, charge model with charge fluxes; ●, polarizable model with charge fluxes.

mations of internal coordinates, i.e., to charge fluxes, as demonstrated here for NH ob deformation.

The next step was to optimize MM charge flux parameters to the electric potentials of the different NH ob configurations to account for the electrostatic changes. The parameters of the different (nonpolarizable and polarizable) models are given in Table 5. Note that the charge parameters in the (previously optimized) polarizable model of NMA are somewhat different from those of the fixed charge model due to the intramolecular electric field.[14]

Because the variations of the CHELPG and Spackman atomic charges as a function of γ all appeared to be linear over a relatively large range of γ (shown for nitrogen in Figure 5), the standard linear expression of eq 2, but with $(r_j - r_{j0})$ replaced by $|\gamma|$, was used in the optimization of charge flux parameters. For very large deformations, of course, the γ dependence cannot be linear. Nor can it be linear for very small deformations, because the planar symmetry of the peptide group would then lead to a V-shaped potential with a discontinuous derivative at $\gamma = 0$. In actual calculations we therefore intend to use the function

$$\Delta q_{b\gamma} = a_{b\gamma}\frac{c_{b\gamma}\gamma^2}{1 + c_{b\gamma}\gamma^2} \qquad (4)$$

where $a_{b\gamma}$ and $c_{b\gamma}$ are constants, to describe the charge flux in bonds containing the center atom of an ob coordinate (i.e., nitrogen in the case of NH ob deformation). This function adequately reproduces the charge variations at the atoms of those bonds for both small and large deformations of γ. The solid curve shown in Figure 5 was obtained with $a_{b\gamma}(\mathrm{CN}) = -0.127$ e, $a_{b\gamma}(\mathrm{NC_m}) = -0.058$ e, $a_{b\gamma}(\mathrm{NH}) = -0.065$ e, and $c_{b\gamma} = 3.0$ rad^{-2} (the last one being the same for all bonds). The Wilson ob angle (in the general case) is not defined at $\gamma = \pi/2$,[20] and in cases where the ob angle may reach $\pm\pi/2$ another type of ob coordinate must be used.[31]

The charge fluxes in the bonds containing the center atom of the ob coordinate may give rise to secondary fluxes in groups that are farther away. This is taken into account in our model by the possibility of defining charge fluxes in bonds that are one bond away from the center atom. In the present case of NMA, these bonds are the CC_m, C═O, and *N*-methyl C_mH bonds. Based on our linear charge flux implementation, it turned out that there is conformational dependence in these secondary charge fluxes. In their optimization we used the expression

$$\Delta q_{b\gamma} = a_{b\gamma}|\gamma| \sin^2 \chi \qquad (5)$$

where χ is the dihedral angle whose arms are bond *b* and the

TABLE 3: Weighted Relative Root-Mean-Square Deviation (in percent) as a Function of the NH Out-of-Plane Angle γ in NMA for a Peptide CN (Bell) Torsion Angle of 15°

	$\gamma = 0°$	$\gamma = 8.7°$	$\gamma = 17.5°$	$\gamma = 26.4°$	$\gamma = 35.6°$	$\gamma = 45.0°$	overall
fixed charges[a]	4.8	5.3	6.5	8.6	11.5	15.5	9.1
charges with charge fluxes[b]	4.5	4.8	5.4	6.0	6.4	7.1	5.7
polarizable[a]	5.2	5.1	5.9	7.8	10.7	14.6	8.5
polarizable with charge fluxes[b]	5.2	4.4	4.3	4.6	5.1	5.8	4.9

[a] Parameters from ref 14. [b] Parameters optimized in this work (see Table 5).

TABLE 4: Weighted Relative Root-Mean-Square Deviations (in percent) as a Function of the Peptide CN (Bell) Torsion Angle ω in NMA[a]

	$\omega = 0°$		$\omega = 5°$		$\omega = 10°$		$\omega = 15°$	
	$\gamma = 0°$	$\gamma = 17.5°$	$\gamma = 0°$	$\gamma = 17.5°$	$\gamma = 0°$	$\gamma = 17.5°$	$\gamma = 0°$	$\gamma = 17.5°$
fixed charges[b]	4.8	5.6	4.5	5.8	4.6	6.1	4.8	6.5
charges with charge fluxes[c]	4.9	5.2	4.6	5.3	4.5	5.3	4.5	5.4
polarizable[b]	4.0	5.1	3.9	5.0	4.4	5.3	5.2	5.9
polarizable with charge fluxes[c]	4.0	4.8	3.9	4.3	4.4	4.1	5.2	4.3

[a] The values are given for two NH out-of-plane angles γ. [b] Parameters from ref 14. [c] Parameters optimized in this work (see Table 5).

TABLE 5: Parameters of Our Nonpolarizable and Polarizable Electrostatic Models of NMA

parameter[a]	nonpolarizable[b]	polarizable[b]
Charge Parameters (BCIs)		
$q(C_mH)$ (*C*-methyl)	0.1844 (18)	0.1776
$q(CC_m)$	−0.1482	−0.1925
q(CN)	−0.0649	−0.0969
$q(NC_m)$	0.1798	0.1029
$q(C_mH)$ (*N*-methyl)	0.0916	0.1443
q(CO)	−0.5692	−0.6766
q(NH)	0.3265	0.3984
Charge Flux Parameters		
$a(C_mH)$[c] (*C*-methyl)	−0.0085 (12)	
$a(CC_m)$[d]	0.0428 (136)	0.0627 (191)
a(CN)	−0.1074 (56)	−0.1211 (93)
$a(NC_m)$	−0.0489 (57)	−0.0578 (72)
$a(C_mH)$[d] (*N*-methyl)	−0.0681 (59)	−0.0793 (65)
a(CO)[d]		−0.0894 (245)
a(NH)	−0.0547 (63)	−0.0349 (65)
Bond Polarizability		
$\alpha(C_mH)$ (*C*-methyl)		0.6470
$\alpha(CC_m)$		0.7648
α(CN)		2.5656
$\alpha(NC_m)$		2.0941
$\alpha(C_mH)$ (*N*-methyl)		0.6238
α(CO)		3.1064
α(NH)		1.1364
Atomic Polarizability		
$\alpha_{pp,C}(C_mH)$ (*C*-methyl)		0.4782
$\alpha_{pp,O}$(CO)		1.0275
$\alpha_{pp,N}$(NH)		1.8969

[a] The units are electrons for charges, radians for angles (for charge fluxes), and angstroms cubed for polarizabilities. All parameters relate to bonds. The atoms of the bond to which a parameter pertains are given in parentheses. C_m denotes sp^3 carbon. The following sign convention is used when calculating atomic charges from BCIs: q(AB) is added to atom B and $-q$(AB) is added to atom A. The same sign convention is used for charge fluxes calculated with eq 2. The notation for polarizability refers to model POL1 in ref 14; i.e., α(AB) is the polarizability of bond AB and $\alpha_{pp,A}$(AB) is the polarizability of atom A in a direction perpendicular to bond AB. [b] Numbers in parentheses are statistical uncertainties of the last digits. Only parameters for which uncertainties are given were optimized in this work. The other parameters were optimized in ref 14. [c] Charge flux in the *C*-methyl C_mH bonds due to CC_m torsion. All other charge fluxes in this table refer to NH ob deformation. [d] Modulation according to eq 5.

bond connecting the center and end atoms of γ (the N and H atoms in NH ob deformation). Again, in actual calculations $|\gamma|$ should be replaced by a function that has a continuous derivative at $\gamma = 0$, such as that of eq 4. Charge fluxes beyond the secondary ones are currently not taken into account in our model.

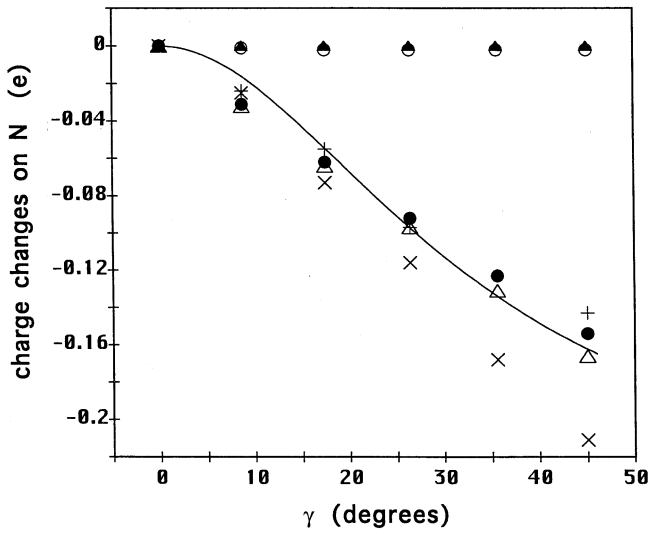

Figure 5. Variation of the nitrogen charge of NMA as a function of the NH out-of-plane angle γ in different electrostatic models. + refers to the CHELPG charges and × to the Spackman charges at the MP2/6-31++G(d,p) density. The solid curve is calculated with eq 4. Other notations are the same as in Figure 4.

All charge flux parameters of the types mentioned above were varied in the optimization. In addition, we also implemented charge flux for the *C*-methyl C_mH bonds as a function of the NCC_mH torsion angle, as suggested by the slightly different CHELPG charges on these hydrogen atoms (see Tables 2 and 5). Note that the *C*-methyl hydrogen CHELPG charges do not vary much with NH ob, in agreement with the results of our optimizations, which show that such distant charge fluxes can be neglected. The resulting atomic charges as functions of the NH ob angle (for $\omega = 15°$) are given in Tables 6 and 7 for our nonpolarizable and polarizable charge flux models, respectively. Due to the nonzero CC_m torsion charge flux in the charge/charge flux model, the *C*-methyl C_mH BCI also had to be reoptimized (see Table 5), whereas all other BCIs were held fixed at their previously determined values.[14] In this model, the charge flux in the C═O bond became very small, with a large uncertainty, and was therefore set to zero. This is in agreement with the CHELPG oxygen charge, which also changes very little. All other primary and secondary charge flux parameters were determinate.

As mentioned above, our indication is that polarization cannot reproduce the variations in the NMA atomic charges caused by

TABLE 6: Atomic Charges (in electrons) of NMA Calculated with Our Nonpolarizable Charge Flux Model at Different NH Out-of-Plane Angles γ for a 15° Peptide CN (Bell) Torsion Angle

atom[a]	$\gamma = 0°$	$\gamma = 8.7°$	$\gamma = 17.5°$	$\gamma = 26.4°$	$\gamma = 35.6°$	$\gamma = 45.0°$
C_m (*C*-methyl)	−0.702	−0.702	−0.704	−0.707	−0.710	−0.716
H	0.189	0.189	0.189	0.189	0.189	0.189
H	0.189	0.189	0.189	0.189	0.189	0.189
H_{ip}	0.176	0.176	0.176	0.176	0.176	0.176
C	0.782	0.799	0.817	0.837	0.858	0.881
O	−0.569	−0.569	−0.569	−0.569	−0.569	−0.569
N	−0.571	−0.603	−0.636	−0.669	−0.702	−0.737
H	0.327	0.335	0.343	0.352	0.361	0.370
C_m (*N*-methyl)	−0.095	−0.072	−0.049	−0.025	0.000	0.025
H_{ip}	0.092	0.091	0.089	0.084	0.074	0.061
H	0.092	0.086	0.083	0.083	0.086	0.089
H	0.092	0.083	0.072	0.060	0.050	0.043

[a] Notation as in Table 2.

TABLE 7: Atomic Charges (in electrons) of NMA Calculated with Our Polarizable Charge Flux Model at Different NH Out-of-Plane Angles γ for a 15° Peptide CN (Bell) Torsion Angle

atom[a]	$\gamma = 0°$	$\gamma = 8.7°$	$\gamma = 17.5°$	$\gamma = 26.4°$	$\gamma = 35.6°$	$\gamma = 45.0°$
C_m (*C*-methyl)	−0.655	−0.655	−0.657	−0.660	−0.665	−0.671
H	0.170	0.170	0.170	0.170	0.171	0.171
H	0.168	0.168	0.167	0.166	0.165	0.164
H_{ip}	0.144	0.144	0.144	0.144	0.145	0.144
C	0.865	0.884	0.905	0.931	0.961	0.996
O	−0.596	−0.596	−0.598	−0.602	−0.609	−0.618
N	−0.561	−0.592	−0.623	−0.653	−0.684	−0.715
H	0.373	0.377	0.382	0.386	0.391	0.395
C_m (*N*-methyl)	−0.372	−0.346	−0.320	−0.295	−0.269	−0.243
H_{ip}	0.133	0.133	0.130	0.124	0.113	0.098
H	0.163	0.157	0.156	0.158	0.163	0.169
H	0.168	0.157	0.144	0.131	0.119	0.111

[a] Notation as in Table 2.

NH ob deformation. However, polarization reproduces reasonably well the differences in the charges on the *C*-methyl hydrogen atoms, eliminating the need for NCC_mH torsion charge flux in the C_mH bonds in this particular model (see Table 5). Instead, nonzero NH ob charge flux in the C═O bond is now required to account for the charge variations in the carbonyl group. The charge flux model with polarization is overall somewhat better than that without polarization at reproducing the ab initio electric potential (see Tables 3 and 4 and Figure 4), and it also better reflects the CHELPG charge fluctuations on the carbonyl carbon and nitrogen atoms (Table 7). The charge variations in the methyl groups, though, are very similarly reproduced by both models. In each case it has to be determined whether polarization can explain charge fluctuations.

In Figure 6 the ab initio electric equipotential lines for the configuration of $\omega = 15°$ and $\gamma = 45°$ are compared with those of the polarizable charge flux model and the fixed charge model in a plane containing the NH bond and perpendicular to the CNC_m plane. The polarizable charge flux model gives a better representation of the ab initio electric potential than does the fixed charge model, for both the shapes and radial distances (from the nearest atoms) of the equipotential lines.

Since in the geometry optimizations the bond lengths and valence angles were not kept fixed, variations in other than the NH ob coordinate could also cause intramolecular charge flow. The bond lengths did not vary much, the largest changes being 0.0014 Å. Variations of 5−6° were seen in the CNC_m angle, as can be expected due to the redundancies between the valence angles around the nitrogen atom and the NH ob angle. CHELPG calculations, in which this bond angle was varied by 3−6° without changing any other internal coordinates of the optimized NMA configurations (except those changing because of the redundancies), were carried out with two different NH ob angles (0° and 35.6°), the CN torsion angle being 15°. Most of the CHELPG charges remained practically unchanged, but those of the carbonyl carbon and the *C*-methyl group experienced some variations. With a ∼3° decrease of the CNC_m angle, the largest charge change occurred for the *C*-methyl carbon atom, of the order of 0.03 e in the planar structure, and less in the deformed structure. Decreasing the angle by another 3°, the charges in the planar structure did not change much, whereas in the deformed structure the charges experienced slightly larger changes. The bond length variations being very small, and because of the redundancies in the valence and out-of-plane bend angles around the center atom of the ob coordinate, it seems to be a reasonable approximation to let these charge fluxes be implicitly included in those resulting from NH ob deformation. However, for calculating IR intensities[22,23] it is necessary to explicitly include the angle and bond charge fluxes. Also, as mentioned earlier, the charges do not change much on moderate deformation of the CN torsion angle, and we have therefore not included CN torsion charge flux in the present study.

4. Conclusions

In this investigation, the goal has been to explore in more detail the electrostatic features, the intrinsic geometries, and the use of proper coordinates in the pyramidalization at the nitrogen atom of the peptide group. Although crucial for the correct dynamics and energetics of the peptide group, these characteristics are not accounted for in any current MM force field for peptides and proteins. The absence of these kinds of explicit details in MM energy functions means that their effects, at least to some degree, will be compensated, but with erroneous physical representations, by other existing terms in the energy function. This also easily leads to nontransferability of structur-

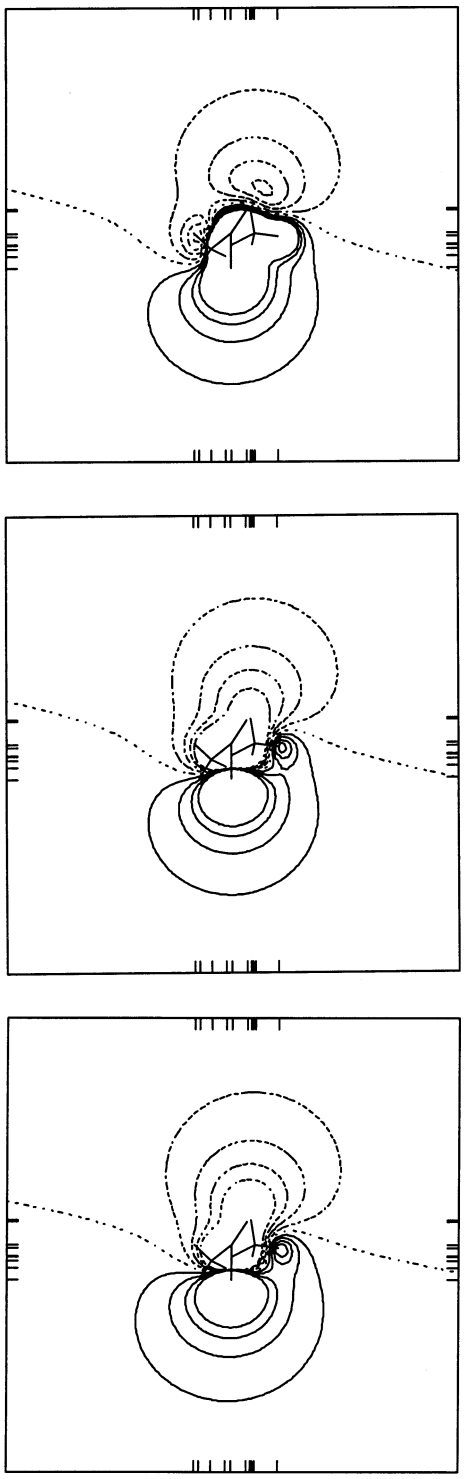

Figure 6. Electric equipotential lines in a plane containing the NH bond and perpendicular to the CNC_m plane of NMA (Figure 1), as given by MP2/6-31++G(d,p) (top), polarizable charge flux model (center), and fixed charge model[14] (bottom). Solid line, positive potential; broken line, negative potential; dotted line, zero potential. The lines are drawn at intervals of 1 kcal mol^{-1} e^{-1}. Lines at borders indicate positions of atoms.

ally closely related MM parameters, good examples being several reoptimizations of torsion potentials in the literature.

A basic requirement for a proper description of nonplanar deformations of the peptide group is the orthogonality of the sp^2-sp^2 peptide CN torsion coordinate and the associated (NH and C=O) out-of-plane deformation coordinates. Such nonredundant coordinates are routinely used in spectroscopic force fields but not yet in regular MM force fields, although the problem has been pointed out.[4−10] In fact, our SDFF[6] is the only modern MM force field in which these coordinates have been implemented. The standard description of sp^2-sp^2 torsions by separate redundant energy terms for all four dihedral angles causes an out-of-plane deformation to also register as a torsion deformation and leads to incorrect potential energy contributions for these coordinates. In addition to the necessity of using such orthogonal coordinates, the results of our studies show that, first, the intrinsic NH ob angle parameter is a significant function of the peptide CN (Bell) torsion angle and cannot be represented, as it is in present standard force fields, by a constant. Second, any pyramidalization at the nitrogen atom is accompanied by large changes in partial charges on some atoms of the peptide group, which means that a Coulomb model with fixed charges is not a good MM representation for electrostatic interactions in this case. Because the charge changes are not accommodated by polarization, they must be represented by charge fluxes, which allow the charges to vary continuously as a function of the NH out-of-plane bend coordinate. We have provided parameters to account for these changes in NMA, and we are studying polypeptide systems to test the transferability of the derived models.

Acknowledgment. This research was supported by NSF Grants MCB9903991 and DMR9902727, and by the Life Science Corridor Fund of the Michigan Economic Development Corporation.

Note Added in Proof. When incorporating the charge fluxes in the energy function, it is important that there be no unbalanced charges in the summation of the Coulomb interactions, since this results in unphysical electrostatic energies. In a recent paper (Palmo, K.; Mannfors, B.; Krimm, S. *Chem. Phys. Lett.* **2003**, *369*, 367−373) we present a method for avoiding this problem.

References and Notes

(1) Buck, M.; Karplus, M. *J. Am. Chem. Soc.* **1999**, *121*, 9645−9658.
(2) Carey, P. *J. Biol. Chem.* **1999**, *274*, 26625−26628.
(3) Dian, B. C.; Longarte, A.; Zwier, T. S. *Science* **2002**, *296*, 2369−2373.
(4) Winkler, F. K.; Dunitz, J. D. *J. Mol. Biol.* **1971**, *59*, 169−182.
(5) Ermer, O.; Lifson, S. *J. Am. Chem. Soc.* **1973**, *95*, 4121−4132.
(6) Mannfors, B.; Sundius, T.; Palmo, K.; Pietila, L.-O.; Krimm, S. *J. Mol. Struct.* **2000**, *521*, 49−75.
(7) Mannfors, B.; Pietila, L.-O.; Palmo, K. *J. Mol. Struct.* **1991**, *248*, 289−316.
(8) Mannfors, B.; Pietila, L.-O.; Palmo, K. *J. Mol. Struct.* **1994**, *328*, 287−295.
(9) Halgren, T. A.; Nachbar, R. B. *J. Comput. Chem.* **1996**, *17*, 587−615.
(10) Maple, J. R.; Hwang, M. J.; Jalkanen, K. J.; Stockfish, T. P.; Hagler, A. T. *J. Comput. Chem.* **1998**, *19*, 430−458.
(11) Palmo, K.; Pietila, L.-O.; Krimm, S. *J. Comput. Chem.* **1991**, *12*, 385−390.
(12) Francl, M. M.; Chirlian, L. E. In *Reviews in Computational Chemistry*; Lipkowitz, K. B., Boyd, D. B., Eds.; Wiley-VHC: New York, 2000; Vol. 14, pp 1−31.
(13) Mannfors, B.; Palmo, K.; Krimm, S. *J. Mol. Struct.* **2000**, *556*, 1−21.
(14) Mannfors, B.; Mirkin, N. G.; Palmo, K.; Krimm, S. *J. Comput. Chem.* **2001**, *22*, 1933−1943.
(15) Frisch, M. J.; Trucks, G. W.; Schlegel, H. B.; Scuseria, G. E.; Robb, M. A.; Cheeseman, J. R.; Zakrzewski, V. G.; Montgomery, J. A., Jr.; Stratmann, R. E.; Burant, J. C.; Dapprich, S.; Millam, J. M.; Daniels, A. D.; Kudin, K. N.; Strain, M. C.; Farkas, O.; Tomasi, J.; Barone, V.; Cossi, M.; Cammi, R.; Mennucci, B.; Pomelli, C.; Adamo, C.; Clifford, S.; Ochterski, J.; Petersson, G. A.; Ayala, P. Y.; Cui, Q.; Morokuma, K.; Malick, D. K.; Rabuck, A. D.; Raghavachari, K.; Foresman, J. B.; Cioslowski, J.; Ortiz, J. V.; Stefanov, B. B.; Liu, G.; Liashenko, A.; Piskorz, P.; Komaromi, I.; Gomperts, R.; Martin, R. L.; Fox, D. J.; Keith, T.; Al-Laham, M. A.; Peng, C. Y.; Nanayakkara, A.; Gonzalez, C.; Challacombe, M.; Gill, P. M. W.; Johnson, B.; Chen, W.; Wong, M. W.; Andres, J. L.; Gonzalez, C.;

Head-Gordon, M.; Replogle, E. S.; Pople, J. A. *GAUSSIAN 98*, Revision A.3; Gaussian, Inc.: Pittsburgh, PA, 1998.

(16) Schmidt, M. W.; Baldridge, K. K.; Boatz, J. A.; Elbert, S. T.; Gordon, M. S.; Jensen, J. H.; Koseki, S.; Matsunaga, N.; Nguyen, K. A.; Su, S. J.; Windus, T. L.; Dupuis, M.; Montgomery, J. A. *J. Comput. Chem.* **1993**, 14, 1347−1363.

(17) Breneman, C. M.; Wiberg, K. B. *J. Comput. Chem.* **1990**, *11*, 361−373.

(18) Spackman, M. A. *J. Comput. Chem.* **1996**, *17*, 1−18.

(19) Palmo, K.; Krimm, S. SPEAR: Spectroscopic Potential Energy Analytical Refinement−A Molecular Parametrization and Modeling Package. To be published.

(20) Wilson, E. B., Jr.; Decius, J. C.; Cross, P. C. *Molecular Vibrations. The Theory of Infrared and Raman Vibrational Spectra*; Dover Publications: New York, 1980.

(21) Bell, B. P. *Trans. Faraday Soc.* **1945**, *41*, 293−295.

(22) Palmo, K.; Krimm, S. *J. Comput. Chem.* **1998**, *19*, 754−768.

(23) Palmo, K.; Mannfors, B.; Mirkin, N. G.; Krimm, S. *Biopolymers* **2003**, *68*, 383−394.

(24) Sigfridsson, E.; Ryde, U. *J. Comput. Chem.* **1998**, *19*, 377−395.

(25) Mirkin, N. G.; Krimm, S. *J. Mol. Struct. (THEOCHEM)* **1995**, *334*, 1−6.

(26) MacArthur, M. W.; Thornton, J. M. *J. Mol. Biol.* **1996**, *264*, 1180−1195.

(27) Ramek, M.; Yu, C.-H.; Sakon, J.; Schäfer, L. *J. Phys. Chem. A* **2000**, *104*, 9636−9645.

(28) Mirkin, N. G. Unpublished data.

(29) Mannfors, B.; Mirkin, N. G.; Palmo, K.; Krimm, S. To be published.

(30) Qian, W.; Mirkin, N. G.; Krimm, S. *Chem. Phys. Lett.* **1999**, *315*, 125−129.

(31) Lee, S.-H.; Palmo, K.; Krimm, S. *J. Comput. Chem.* **1999**, *20*, 1067−1084.